Homogeneous nucleation rate measurements of 1-propanol in helium: The effect of carrier gas pressure

ARTICLE *in* THE JOURNAL OF CHEMICAL PHYSICS · MAY 2006

Impact Factor: 2.95 · DOI: 10.1063/1.2185634 · Source: PubMed

3 AUTHORS, INCLUDING:

Vladimír Ždímal
Academy of Sciences of the Czech Republic
98 PUBLICATIONS **966** CITATIONS

SEE PROFILE

Homogeneous nucleation rate measurements of 1-propanol in helium: The effect of carrier gas pressure

David Brus[a] and Vladimír Ždímal
Laboratory of Aerosol Chemistry and Physics, Institute of Chemical Process Fundamentals, Academy of Sciences of the Czech Republic, Rozvojová 135, 165 02 Prague 6, Czech Republic

Frank Stratmann
Institute for Tropospheric Research, 704318 Leipzig, Germany

(Received 27 December 2005; accepted 15 February 2006; published online 25 April 2006)

Kinetics of homogeneous nucleation in supersaturated vapor of 1-propanol was studied using an upward thermal diffusion cloud chamber. Helium was used as a noncondensable carrier gas and the influence of its pressure on observed nucleation rates was investigated. The isothermal nucleation rates were determined by a photographic method that is independent on any nucleation theory. In this method, the trajectories of growing droplets are recorded using a charge coupled device camera and the distribution of local nucleation rates is determined by image analysis. The nucleation rate measurements of 1-propanol were carried out at four isotherms 260, 270, 280, and 290 K. In addition, the pressure dependence was investigated on the isotherms 290 K (50, 120, and 180 kPa) and 280 K (50 and 120 kPa). The isotherm 270 K was measured at 25 kPa and the isotherm 260 K at 20 kPa. The experiments confirm the earlier observations from several thermal diffusion chamber investigations that the homogeneous nucleation rate of 1-propanol tends to increase with decreasing total pressure in the chamber. In order to reduce the possibility that the observed phenomenon is an experimental artifact, connected with the generally used one-dimensional description of transfer processes in the chamber, a recently developed two-dimensional model of coupled heat, mass, and momentum transfer inside the chamber was used and results of both models were compared. It can be concluded that the implementation of the two-dimensional model does not explain the observed effect. Furthermore the obtained results were compared both to the predictions of the classical theory and to the results of other investigators using different experimental devices. Plotting the experimental data on the so-called Hale plot shows that our data seem to be consistent both internally and also with the data of others. Using the nucleation theorem the critical cluster sizes were obtained from the slopes of the individual isotherms and compared with the Kelvin prediction. The influence of total pressure on the observed isothermal nucleation rate was studied in another experiment, where not only temperature but also supersaturation was kept constant as the total pressure was changed. It was shown that the dependence of the nucleation rate on pressure gets stronger as pressure decreases. © *2006 American Institute of Physics*. [DOI: 10.1063/1.2185634]

INTRODUCTION

Homogeneous vapor-to-liquid nucleation is the formation of a liquid phase from a pure vapor and belongs to the first order phase transitions. The nucleation process occurs due to a density fluctuation of molecules present in the vapor which thereon leads to a random formation of small clusters.

It was assumed for a long time that the presence of a noncondensable carrier gas does not influence the clustering process. The only role of the carrier gas was to keep clusters in thermal equilibrium with its surroundings, so the process can be treated as isothermal.

However, there is experimental evidence suggesting that homogeneous nucleation kinetics does depend on the type and amount of carrier gas. As early as 1956, Franck and Hertz[1] made such observations in ethanol vapor using a thermal diffusion cloud chamber (TDCC). They reported that the critical supersaturation increased with increasing total pressure, i.e., the nucleation rate decreased with increasing pressure. Their result was forgotten for a long time. In the late 1980s new studies pointing out the influence of carrier gas pressure on nucleation appeared.

In TDCCs, a decrease of nucleation rate with increasing total pressure was repeatedly observed, both in the range of nearly atmospheric pressures [Katz *et al.*[2] (1988) and Ždímal *et al.*[3] (1995)] and at elevated pressures [Chukanov *et al.*[4] (1989), Heist *et al.*[5] (1994), Heist *et al.*[6] (1995), and other papers of Heist's group]. Despite this, Strey's group, in their expansion chamber, did not observe any influence of carrier gas on nucleation [Viisanen and Strey[7] (1994) and Viisanen *et al.*[8] (1993)] with one exception [van Remoortere *et al.*[9] (1996)], but there the authors reported a very weak dependence with opposite sign. Anisimov *et al.*,[10] in a flow diffusion chamber, reported a significant increase of nucleation rate with increasing total pressure. On the other hand

[a]Electronic mail: brus@icpf.cas.cz

Hyvärinen *et al.*[11] observed in a flow diffusion chamber the same dependency of nucleation rate on total pressure as found in TDCCs. Luijten *et al.*,[12–14] in a shock tube experiment, also observed a rather strong increase of nucleation rate with increasing pressure in the range of elevated pressures (10–40 bars), but in their work the effect is explained by the decrease of surface tension due to adsorption of nitrogen on the cluster surface. Graßmann and Peters[15] (2001) in their piston-expansion tube observed that the nucleation rate may also depend on the depth of expansion in their device; the authors suggested that this effect is probably caused by fast heat conduction from the tube walls to its central part where the measurements were performed.

Theoreticians have been trying to explain the observed effect since the beginning of the 1990s. Ford[16] corrected the classical nucleation theory for a nonideal behavior of vapor-gas mixture and found a rather weak decrease of nucleation rate with increasing pressure. Also Oxtoby and Laaksonnen,[17] treating the problem as a binary nucleation, concluded that the pressure effect is weak and in the same direction as suggested by Ford. Kashchiev[18] also corrected classical theory for gas nonidealities but concluded that an increase in total pressure may stimulate the nucleation process under some conditions, but under different conditions nucleation may be suppressed. Novikov *et al.*[19] studied this effect by a Monte Carlo simulation and found a strong decrease of nucleation rate with increasing pressure, though only for dense carrier gases. Their effect had the same magnitude as the one observed in TDCCs, but their prediction concerning the effect of carrier gas (He, H_2) is in contradiction with experimental observation by Heist *et al.*[5] A completely different approach to this problem was suggested by Itkin.[20] Assuming that nucleation kinetics is controlled by diffusion of the vapor molecules toward the cluster surface, he formulated a theory and outlined a new experiment for TDCC by which his theory might be proven. Levdanski *et al.*[21] (2002) suggested a joint influence of two possible mechanisms by which the carrier gas can effect the nucleation rate. As the gas molecules are adsorbed at the cluster surface, they may hinder the incorporation of vapor molecules into the condensed phase due to blocking the surface. This would lead to the decrease of the deposition rate. On the other hand, the adsorbed molecules lower surface tension, which leads to the decrease of the evaporation rate and hence to the increase of the net flux of vapor molecules onto a cluster.

Several conclusions can be drawn from the preceding paragraphs. There are many contradictions between the theoretical predictions and experimental observations of the pressure effect on nucleation. The comparison of theoretical predictions show that they mostly agree with respect to the sign of the pressure effect (decrease of nucleation rate with increasing pressure) but differ in the predicted magnitude of the effect. Comparing experimental findings a disagreement is found even in sign, covering all possibilities: no effect, increase, or decrease of rate with pressure. Even though these results may sound disqualifying for nucleation experimentalists, it should still be kept in mind what kind of effect is being revealed. On one side temperature and supersaturation influence the homogeneous nucleation rate dramatically: An increase of either 3% in supersaturation or 3 K (about 1%) in temperature causes an increase of homogeneous nucleation rate by factor of 10, while the changes of mass and heat fluxes in the chamber are small. The magnitude of the pressure effect is much weaker, e.g., Ždímal *et al.*[3] (1995) reported a factor of 1000 change in rate by tripling the total pressure (300% change), but such change in pressure induces a very important change in fluxes. It means that both the experiment and the evaluation procedure have to be designed and carried out very carefully. Usually the determination of the nucleation rate itself does not cause a problem; more important is the correct determination of temperature and supersaturation at the spot where the rate is measured. Direct measurement is not possible since the vapor is supersaturated.

Because the pressure effect was observed almost only with devices based on nonisothermal diffusion (static and flow diffusion chambers), there were some concerns within the nucleation community whether the pressure effect is not an experimental artifact. The answer was sought in three main directions.

Calculations of coupled mass and heat transport in the chamber require knowledge of a consistent set of transport parameters of the vapor-gas mixture studied (thermal conductivities, viscosities, binary diffusion coefficient, and a thermal diffusion ratio). In most cases, some of these parameters are missing or at least not known in the temperature range required, and the estimation methods lack precision. To overcome this, an approach based on the kinetic theory of gases has been developed that allows us to find sound potential parameters for the vapor-gas mixture and to calculate all transport parameters in a consistent manner [Ždímal, (1998)].[22] However, applying these transport parameters did not explain the observed pressure effect.

In another study, Fisk and Katz[23] introduced nonidealities of the vapor-gas mixture into their calculations. It was shown that even though these effects are not negligible, they mostly compensate each other (for the case of thermal diffusion cloud chamber) by being implemented consistently in theory and experiment. This means that implementing the nonidealities of the vapor-gas mixture into the calculations does not explain the pressure effect.

In order to calculate the profiles of temperature and supersaturation in the chamber, it is assumed that the chamber is sufficiently "flat," so that a one-dimensional (1D) model can be used for the description of the transport processes in the central part of the chamber. The major concern is that the heated chamber wall (it is often heated to be kept clean of condensate) may cause a buoyancy driven convection that can propagate towards the center of the chamber and cause a slow motion of the gas mixture which might not be detectable on the droplet trajectories. In this case, the rates measured would correspond to temperatures and supersaturations different from those calculated by the 1D model. To test this hypothesis, a couple of models have been developed. Bertelsmann and Heist[24] (1997) formulated a two-dimensional (2D) model of mass and heat transport in connection with their nucleation studies under elevated pressures. Their

model did not include the buoyancy driven convective flow but could be used for testing the instability of the vapor-gas mixture as it starts in the close vicinity of the wall. Ferguson and Nuth[25] (1999) formulated a 2D model of coupled heat, mass, and momentum transfer in TDCCs. They did a parametric study and provided general guidelines for minimization of buoyancy driven convection. In their later paper Ferguson *et al.*[26] (2001) did also comment on the carrier gas effect. Independently, the authors of this paper developed another 2D model of coupled mass, heat, and momentum transport in TDCCs and presented first results [Stratmann *et al.*[27] (1999) and Stratmann *et al.*[28] (2001)].

In this paper new experimental data on the homogeneous nucleation kinetics in the 1-propanol-He system will be presented and analyzed mainly concerning the observed pressure effect.

There are two approaches to study the pressure effect on nucleation kinetics in a TDCC. One of them presented here relies on precise determination of isothermal nucleation rate as a function of supersaturation. The chamber applied here is not suitable for work at pressures much higher than atmospheric, so the available pressure range is quite narrow due to limits of stable operation. However, the method is so sensitive that it allows one to study the pressure effect very well. Another approach is to substantially extend the range of pressures above the atmospheric. In that case even measurements of the so-called critical supersaturations are sensitive enough to observe the pressure effect; only the requirements on chamber construction and safety are much stronger. In addition to that, the 2D effects need to be considered by applying the more detailed model. Also, as the real gas effects are more pronounced at elevated pressures, it becomes necessary to properly implement the pressure dependence of transport parameters into that model. This type of experiments and evaluation had already been carried out in vapors of various compounds and in more than one laboratory, and the observed pressure effect was reported repeatedly.[4–6]

EXPERIMENTAL SETUP AND DATA EVALUATION METHOD

The TDCC used in these experiments is presented in detail elsewhere [e.g., Ždímal and Smolík (1998)].[29] The method used for the data evaluation in the TDCC has been also described in detail elsewhere [Brus *et al.* (2005)].[30] This method gives $J_{exp}(z)dz$, the experimentally determined homogeneous nucleation rate as a function of vertical position inside the chamber, z. The local values of nucleation rate are related to the corresponding local values of temperature and supersaturation calculated using either a traditional 1D model of mass and heat transport [Katz and Ostermier[31] (1967) and Smolík and Ždímal[32] (1994)] or a more recent 2D model of mass, heat, and momentum transfer in the TDCC [e.g., Stratmann *et al.* (2001)].[28] The resulting dependence $J_{exp}(T,S)$ can be directly compared to the theoretical prediction of any nucleation theory.

The thermodynamic parameters of 1-propanol-helium system which are needed to solve the transport equations are presented in Table I.

RESULTS AND DISCUSSION

The homogeneous nucleation rate measurements of 1-propanol-helium system are listed in Table II for all measured isotherms 260, 270, 280, and 290 K. The pressure dependence of the rate was measured for the isotherm 290 K (50, 120, and 180 kPa) and the isotherm 280 K (50 and 120 kPa). Only one pressure was measured for the isotherms 270 K (25 kPa) and 260 K (20 kPa). The isotherms were chosen with a step of 10 K, in the range that could be reasonably well covered by the experimental setup used in this work. In order to suppress the buoyancy driven convection of the vapor-gas mixture inside the TDCC, the total pressure should remain below a limiting value that depends on the temperature, condensable vapor, and background gas. Several criteria were formulated in the course of time [Katz[33] (1970), Bertelsmann and Heist[34] (1997), and Bertelsmann and Heist (part II)[35] (1997)]. We tried to fulfill the strictest ones formulated in the latter paper.

Experimental nucleation rates

The experimental homogeneous nucleation rates ranged from 10^{-1} to 10^{2} drops cm^{-3} s^{-1}. The lower limit is due to difficulties in running the experiments in the steady state for a long time (many hours), and the higher limit is due to vapor depletion and heat release by condensation.

In Fig. 1 the experimental nucleation rates as a function of supersaturation are shown. The shift in the data on isotherm 290 K due to the different pressure levels is clearly visible. The steps among the pressure levels applied are almost equivalent. The difference in nucleation rates on isotherms 290 K at 50 kPa and 290 K at 120 kPa is about one and a half order in magnitude. On the other hand there is almost no difference between isotherms carried out at 120 and 180 kPa; they are practically on one line.

At isotherm 280 K, the nucleation rates measured at total pressure of 50 kPa were about three times higher than those measured at total pressure of 120 kPa.

The isotherm 260 K shows more scatter in the lower part because of slight instability in the temperature measurement and an increased uncertainty in experimental nucleation rate determination. The instability was caused by the moisture in the room air condensing on the upper plate heat exchanger (even though the exposed surfaces of the exchanger were continuously washed by dry nitrogen).

Comparison between 1D and 2D models

The experimental nucleation rate data as a function of supersaturation are plotted in Fig. 2; the data calculated by the 1D model are represented by solid symbols and the data obtained using the 2D model are represented by open symbols of the same shape. Only selected experimental points were processed by the 2D model.

It is evident from Fig. 2 that it is impossible to explain the observed difference between experimental results ob-

TABLE I. Thermodynamic properties. Subscript v=vapor, subscript g=gas, subscript vg=vapor-gas mixture, M=molar mass, T_b=boiling temperature, T_c=critical temperature, P_c=critical pressure, V_c=critical volume, Ω=Pitzer acentric factor, μ=dipole moment, ΔH=enthalpy of vaporization, p_{eq}=equilibrium vapor pressure, γ=surface tension, c_p=heat capacity, λ=thermal conductivity, D=diffusion coefficient, η=viscosity, α =thermal diffusion factor, and ρ=density.

Property	1-propanol	Unit	Ref.
M_v	60.096	kg kmol^{-1}	
T_b	370.4	K	
T_c	536.8	K	47
P_c	5.169×10^{6}	Pa	47
V_c	2.18×10^{-1}	m^3 kmol^{-1}	
Ω	0.624	1	47
μ	1.58	D	47
σ_v	4.549×10^{-10}	m	
ε_v/k	576.70	K	
$c_{p,v}$	$2470.2+3.3252\times10^{2}T-1.8552\times10^{-1}T^2+4.2957\times10^{-5}T^3$	J kmol^{-1}	48
λ_v	$418.68\{6.198\,13\times10^{-5}[\exp(8.645\,42\times10^{-5}T)-\exp(-4.494\,13\times10^{-4}T)]+2.460\,71\times10^{-10}T^2\}$	K^{-1} W m^{-1} K^{-1}	49
λ_l	$1.628\times10^{-1}-2.34\times10^{-4}(T-273.15)$	W m^{-1} K^{-1}	48
$\log\eta_v$	$951.04(1/T-1/327.83)\times10^{-3}$	Pa s	49
ρ_l	$820.1-0.8183(T-273.15)+1.08\times10^{-3}(T-273.15)^2+16.5\times10^{-6}(T-273.15)^3$	kg m^{-3}	50
γ_l	$2.528\times10^{-2}-8.394\times10^{-5}(T-273.15)$	N m^{-1}	50
P_v^{eq}	$133.322\exp(84.6957-8559.6064/T-9.29\ln T)$	Pa	51
ΔH_v	$41.756\times10^{6}((T_c-T)/(T_c-T_b))^{0.38}$	J kmol^{-1}	49
Property	**Helium**	**Unit**	**Ref.**
M_g	4.0026	kg kmol^{-1}	
σ_g	2.551×10^{-10}	m	
ε_g/k	10.22	K	
$c_{p,g}$	5200	J kg^{-1} K^{-1}	48
λ_g	$(-5.8543\times10^{-5}+2.686\,06\times10^{-6}T-7.001\,13\times10^{-9}T^2+1.073\,96\times10^{-11}T^3-6.017\,68\times10^{-15}T^4)\times4.1868\times100$	W m^{-1} K^{-1}	52
η_g	$1.4083\times10^{-6}T^{1.5}/(T+70.22)$	Pa s	52
Property	**1-propanol in helium**	**Unit**	**Ref.**
D_{vg}	$2.663\times10^{-22}T^{1.5}((M_v+M_g)/(2M_vM_g))^{0.5}/(P\sigma_{vg}^2\Omega_{vg}^{(1,1)}\times(kT/\varepsilon_{vg}))$	m^2 s^{-1}	48
$1/\alpha$	$[-0.622\,64+T/(-23.4305+0.305\,37T)](y+0.1548)+0.0964$		53
λ_{vg}	$x_v\lambda_v/(x_v+A_{vg}x_g)+x_g\lambda_g/(x_g+A_{gv}x_v)$	W m^{-1} K^{-1}	48
σ_{vg}	3.550×10^{-10}	m	
ε_{vg}/k	76.77	K	

tained at different levels of total pressure by applying the two-dimensional model of mass, heat, and momentum transport that includes the influence of the heated chamber wall. It might be argued that in the case of isotherm 280 K the use of 2D model puts points measured at different levels of total pressure so close together that it is difficult to discern among them when we take into account the usual experimental uncertainty. However, in the case of the isotherm 290 K the application of 2D model did not help.

Moreover the experiments carried out at 50 kPa are less sensitive to influences from the heated wall than experiments at 120 kPa. Velocity vectors of such experiments are displayed in Fig. 3, pressure of 50 kPa, and in Fig. 4, pressure of 120 kPa. The velocity vectors are characterized by length and direction. The vectors at lower pressure are longer with the upward direction, because the mass and energy fluxes are higher in that case. The vectors corresponding to higher pressure are shorter with a significant change in direction towards the heated wall in the lower part of the chamber and towards the center of the chamber at chamber upper part. Particularly important is the fact that the region of comparison, i.e., 10% of R around the symmetry axis of the chamber, does not seem to be significantly affected at any of the two pressure levels.

Comparison with theory

The critical cluster sizes can be determined from the slopes of the nucleation rate isotherms according to the nucleation theorem [Kashchiev[36] (1982) and Anisimov and Cherevko[37] (1983)]:

TABLE II. The nucleation rates of 1-propanol in helium. T_b is temperature of the bottom plate, T_t is temperature of the top plate, T_{nucl} is nucleation temperature, p_{tot} is total pressure, S_{nucl} is the supersaturation at T_{nucl}, and J_{exp} is the experimental nucleation rate.

T_b (K)	T_t (K)	T_{nucl} (K)	p_{tot} (kPa)	S_{nucl}	J_{exp} (cm^{-3} s^{-1})
		T=260 K, p=20 kPa			
292.43	250.01	260	39.9	3.71	1.23E1
292.31	249.93	260	39.8	3.71	7.50E0
291.53	249.91	260	21.3	3.76	1.68E1
291.46	249.91	260	21.3	3.75	1.17E1
289.39	248	260	21.2	3.71	5.29E0
289.34	248.04	260	21.2	3.70	3.95E0
289.23	248.04	260	21.2	3.68	3.17E0
289.15	248.02	260	21.2	3.66	2.89E0
289.01	248.2	260	19.4	3.64	7.27E−1
288.86	248.24	260	19.4	3.60	8.32E−1
288.7	248.19	260	19.4	3.58	1.41E0
288.72	248.32	260	19.3	3.56	1.18E0
288.53	248.3	260	19.3	3.53	5.96E−1
289.64	248.11	260	19.6	3.77	3.61E1
289.56	248.01	260	19.6	3.77	3.37E1
		T=270 K, p=25 kPa			
300.82	259.66	270	20.4	3.29	7.59E0
300.95	259.52	270	24.2	3.27	4.21E0
300.8	259.53	270	24.2	3.24	3.24E0
300.77	259.52	270	24.2	3.24	3.22E0
300.73	259.55	270	24.2	3.23	2.89E0
300.63	259.5	270	26.1	3.20	1.23E0
300.51	259.55	270	26.1	3.17	9.61E−1
300.43	259.59	270	26.1	3.15	1.24E0
300.28	259.67	270	23.9	3.15	1.13E0
299.94	259.48	270	22.6	3.15	1.21E0
299.96	259.48	270	22.7	3.15	1.29E0
300.04	259.49	270	22.7	3.16	1.01E0
300.31	259.41	270	23.9	3.19	1.64E0
300.37	259.41	270	23.9	3.20	2.46E0
300.5	259.38	270	23.9	3.23	3.27E0
300.55	259.41	270	23.5	3.23	4.34E0
300.6	259.39	270	23.5	3.24	2.96E0
300.68	259.31	270	23.5	3.27	5.56E0
300.76	259.31	270	23.5	3.28	8.76E0
300.85	259.39	270	22.9	3.29	9.97E0
300.9	259.37	270	22.9	3.30	1.23E1
300.98	259.34	270	22.9	3.32	2.00E1
301.04	259.28	270	22.9	3.34	3.30E1
		T=280 K, p=50 kPa			
310.55	267.13	280	49.4	2.98	9.84E0
310.49	267.2	280	49.3	2.97	7.11E0
310.35	267.31	280	49.3	2.94	3.33E0
310.28	267.34	280	48.0	2.93	2.84E0
310.11	267.44	280	48.0	2.90	1.36E0
310.12	267.31	280	49.9	2.91	1.73E0
309.94	267.54	280	49.9	2.86	5.32E−1
309.89	267.56	280	49.6	2.85	3.91E−1
309.89	267.66	280	49.5	2.84	5.69E−1
		T=280 K, p=120 kPa			
312.24	266.45	280	112.3	3.07	1.59E1
311.5	266.71	280	111.2	2.95	9.08E0
312.22	266.46	280	112.4	3.07	3.98E2
311.59	266.59	280	122.3	2.96	1.18E1
311.46	266.57	280	122.2	2.95	1.29E0

TABLE II. (*Continued.*)

T_b (K)	T_i (K)	T_{nucl} (K)	p_{tot} (kPa)	S_{nucl}	J_{exp} (cm^{-3} s^{-1})
		T=280 K, p=120 kPa			
311.42	266.6	280	121.5	2.94	8.80*E*−1
311.25	266.55	280	121.2	2.93	4.67*E*−1
311.41	266.63	280	115.8	2.95	1.38*E*0
311.64	266.63	280	117.6	2.97	2.74*E*0
311.58	266.65	280	117.4	2.96	2.22*E*0
312.44	266.44	280	112.5	3.10	3.53*E*1
311.26	266.47	280	125.4	2.93	1.36*E*0
312.04	266.54	280	112.2	3.04	1.12*E*1
312	266.52	280	111.7	3.04	7.51*E*0
311.85	266.59	280	111.6	3.01	5.32*E*0
311.84	266.61	280	111.5	3.01	4.41*E*0
311.08	266.4	280	120.3	2.93	1.01*E*0
310.82	266.46	280	120.0	2.89	3.53*E*−1
311.06	266.53	280	119.2	2.91	2.83*E*−1
		T=290 K, p=50 kPa			
322.06	278.64	290	50.8	2.69	6.95*E*1
321.94	278.76	290	50.8	2.66	3.52*E*1
321.76	278.79	290	50.6	2.64	1.92*E*1
321.57	278.83	290	50.5	2.62	1.07*E*1
320.8	279.32	290	47.5	2.51	1.36*E*0
320.91	279.74	290	50.3	2.47	5.91*E*−1
320.42	278.5	290	51.0	2.55	2.70*E*0
321.65	279.64	290	50.1	2.54	2.00*E*0
321.71	279.56	290	50.4	2.56	1.27*E*0
322.44	280.5	290	51.3	2.51	8.96*E*−1
320.98	279.24	290	48.6	2.53	1.15*E*0
320.68	277.35	290	50.2	2.68	9.34*E*1
		T=290 K, p=120 kPa			
322.67	276.83	290	120.4	2.74	1.57*E*0
322.5	276.86	290	120.2	2.72	1.15*E*0
322.35	276.93	290	120.1	2.70	1.37*E*0
322.52	276.88	290	120.0	2.72	1.26*E*0
322.32	276.99	290	119.4	2.69	4.64*E*−1
322.16	277.09	290	119.2	2.66	7.10*E*−1
322.06	277.21	290	119.3	2.64	4.11*E*−1
322.89	277.05	290	119.3	2.74	3.36*E*0
322.99	277.1	290	119.3	2.74	5.09*E*0
323.1	276.97	290	121.5	2.76	4.04*E*0
324.14	277.65	290	123.1	2.79	3.08*E*1
324.09	277.73	290	122.5	2.78	1.97*E*1
323.9	277.89	290	122.7	2.74	8.08*E*0
323.47	277.97	290	122.4	2.69	1.10*E*0
322.91	278.1	290	118.6	2.63	7.87*E*−2
322.2	276.15	290	117.6	2.76	1.09*E*1
321.81	276.19	290	117.4	2.72	3.58*E*0
321.71	276.23	290	117.3	2.70	1.21*E*0
		T=290 K, p=180 kPa			
322.01	275.99	290	176.6	2.68	8.59*E*−1
324.66	277.9	290	198.8	2.71	1.79*E*0
323.08	276.54	290	177.4	2.73	2.14*E*0
322.41	275.85	290	177.0	2.73	3.63*E*0
322.58	275.86	290	178.9	2.74	4.26*E*0
323.41	276.58	290	180.2	2.75	4.47*E*0
322.67	275.83	290	179.0	2.75	6.61*E*0
322.77	275.81	290	179.1	2.77	1.01*E*1
322.86	275.76	290	179.2	2.78	1.20*E*1
323.01	275.75	290	179.4	2.79	2.92*E*1

TABLE II. (*Continued.*)

T_b (K)	T_t (K)	T_{nucl} (K)	p_{tot} (kPa)	S_{nucl}	J_{exp} (cm^{-3} s^{-1})
		T=290 K, p=180 kPa			
323.08	275.72	290	179.6	2.80	3.99*E*1
321.87	276.02	290	178.1	2.66	1.32*E*0
323.21	276.94	290	177.0	2.70	1.96*E*0
321.88	276.01	290	175.2	2.66	1.42*E*0
323.32	275.9	290	199.0	2.79	1.26*E*1
323.4	276.44	290	180.5	2.76	1.26*E*1
323.44	275.79	290	199.1	2.81	3.02*E*1
323.19	275.92	290	198.8	2.78	3.00*E*1

$$\left(\frac{\partial \ln J}{\partial \ln S}\right)_T \approx n^*. \tag{1}$$

In Eq. (1) n^* is the number of molecules in the critical cluster. The theoretical radius of the critical cluster r^* can be obtained from the Kelvin equation:

$$r^* = \frac{2\sigma v_{liq}}{kT \ln S}, \tag{2}$$

where v_{liq} is the volume of the spherical cluster that has the same volume per molecule as the bulk liquid and S is the experimental supersaturation. According to the Kelvin equation, the critical cluster size depends both on temperature and supersaturation. The number of molecules in the critical clusters, as determined from the experimental data (symbols) and the Kelvin equation (solid line), is presented in Table III and Fig. 5. The supersaturation is taken at the middle of each isotherm at the rate of 3 drops cm^{-3} s^{-1}.

The predicted values of critical cluster size highly overestimate the values obtained from slopes of the nucleation rate isotherms. Also the differences among the same isotherms but at different pressure levels can be clearly seen. The highest difference is at isotherm 290 K carried out at 50 kPa. The value determined from the experimental data is about 70 molecules less than that predicted by the Kelvin equation.

The molecular content of the experimental critical cluster values is slightly smaller as supersaturation goes higher (or temperature goes lower). The exceptions to this trend are the isotherms 290 K at 50 kPa and 260 K at 20 kPa. The isotherm 290 K at 50 kPa has the shallowest slope from isotherm 290 K. The isotherm 260 K is close to the lower applicable temperature limit of the chamber. At this isotherm the upper plate working temperature is 248 K and the moisture in the room air condenses on the upper plate heat exchanger (even when blowing dry nitrogen towards the exposed surfaces to suppress the water condensation) causing a slight instability in the temperature measurement and also an increased uncertainty in experimental nucleation rate determination.

The experimental nucleation rates as a function of supersaturation are shown in Fig. 6 together with the nucleation rates predicted by the classical nucleation theory [Becker and Döring (1935)].[38] It is often stated about the classical theory that while it fails to predict correctly the temperature dependency of nucleation rate, its prediction of the supersaturation dependency is good. However, as we have seen on the criti-

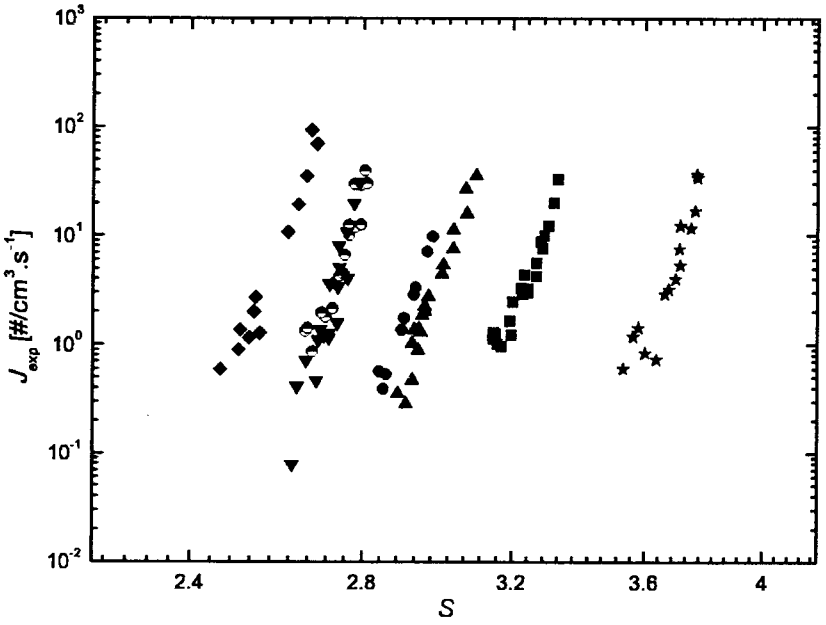

FIG. 1. The experimental nucleation rates J_{exp} as a function of supersaturation S of 1-propanol. The isotherm 290 K at three levels of pressure 50, 120, and 180 kPa, the isotherm 280 K at two levels of pressure 50 and 120 kPa, the isotherm 270 K at 25 kPa, and isotherm 260 K at 20 kPa.

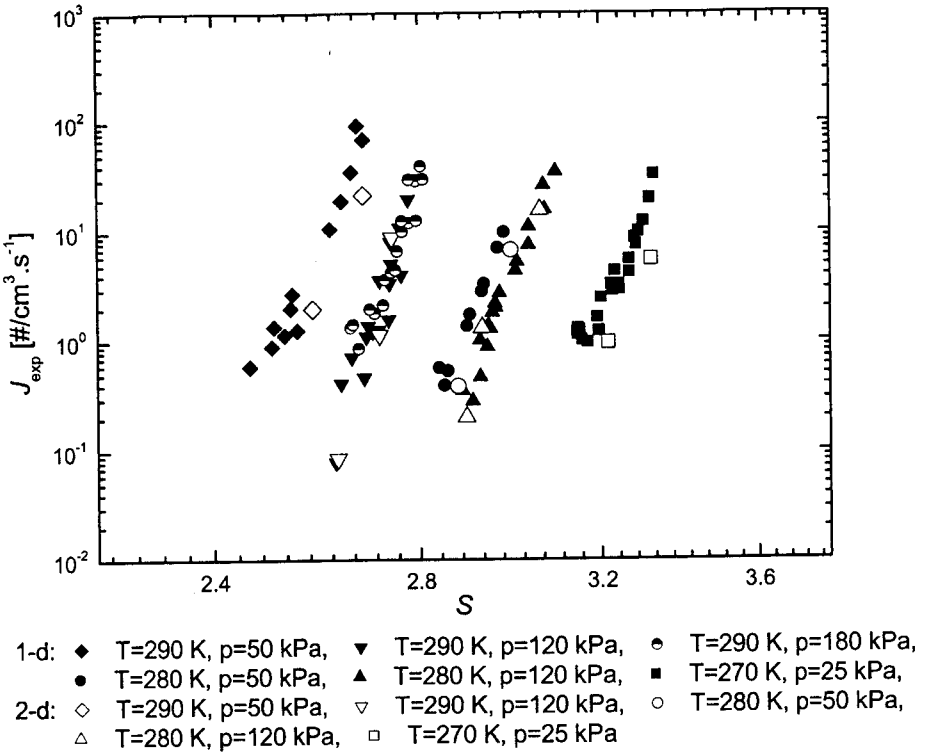

FIG. 2. The experimental nucleation rates J_{exp} as a function of supersaturation S of 1-propanol. The comparison of experimental data obtained using one-dimensional model (solid symbols) and two-dimensional model (open symbols).

cal cluster size analysis, the predictive force of classical theory concerning the supersaturation dependency is not perfect as well.

Concerning relative positions of the isotherms, it seems that there is a generally observed trend: Towards low temperatures (i.e., high supersaturation) the theoretical supersaturations are above the experimental ones while on the high temperature side (i.e., low supersaturations) the opposite is true. As a consequence there has to be a crossover point where theory and experiment match exactly. In Fig. 6 this would be approximately at 275 K.

Performing a quantitative comparison, the theoretically predicted values of nucleation rate of isotherm 260 K underestimate the experimental values about a factor of 5. The experimental values of isotherm 270 K are about a quarter of order in magnitude higher than the predicted values. The theoretically predicted values of nucleation rate of isotherm 280 K slightly overestimate the experimental values of isotherm 280 K carried out at 120 kPa. The experimental values of isotherm 280 K at 50 kPa have almost the same position as theoretical prediction but feature a different slope. The theoretically predicted isotherm 290 K lies between experi-

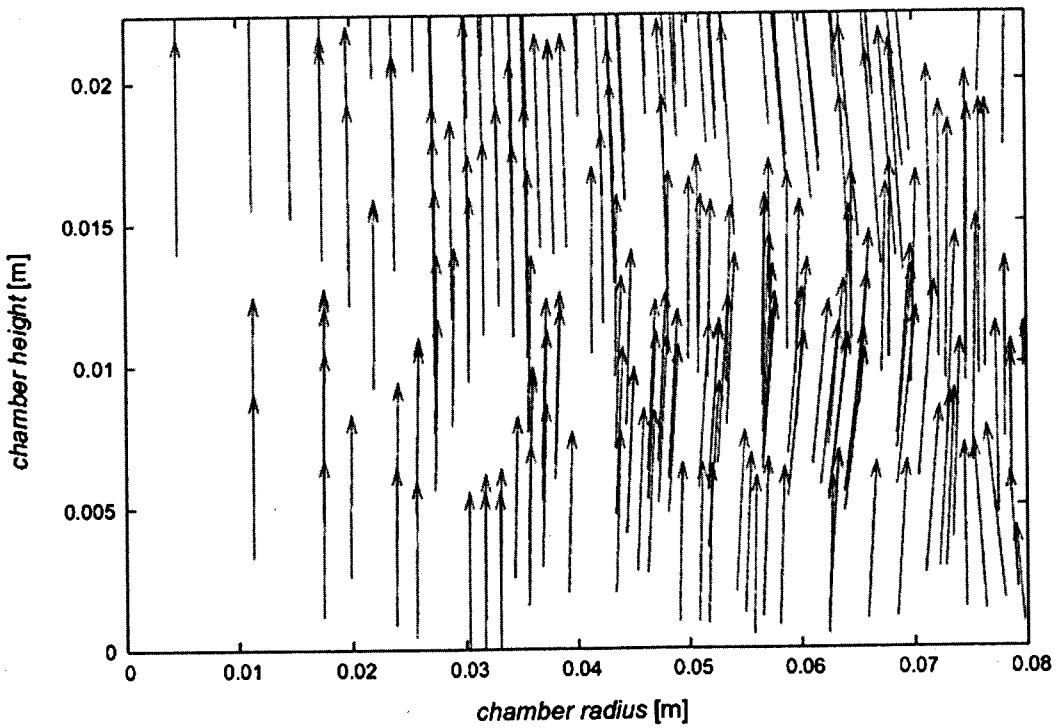

FIG. 3. The velocity vectors of isotherm 290 K at 50 kPa inside TDCC obtained by two-dimensional model.

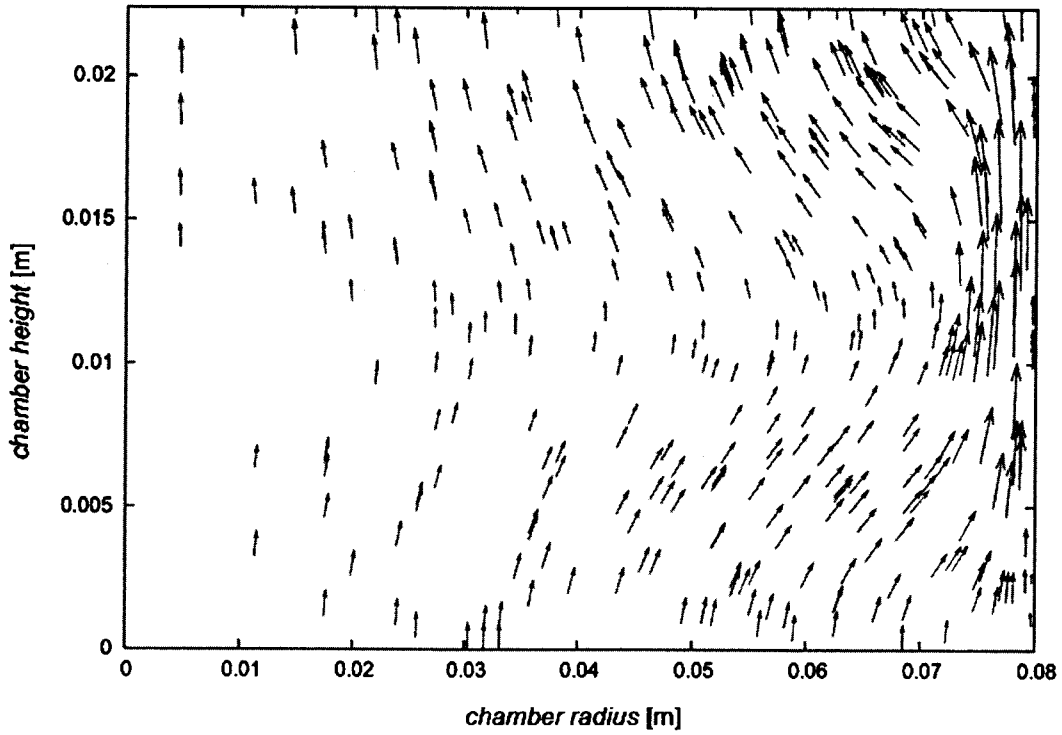

FIG. 4. The velocity vectors of isotherm 290 K at 120 kPa inside TDCC obtained by two-dimensional model.

mental data of isotherms 290 K carried out at 120 and 180 kPa on the right side and experimental data of isotherm 290 K at 50 kPa on the left side. The predicted isotherm 290 K has a different slope than all the experimental 290 K isotherms. The predicted isotherm 290 K is at the upper part closer to data of the experimental isotherm 290 K at 50 kPa and at lower part closer to the isotherm 290 K at 120 and 180 kPa.

Comparison with other measurements

In this section only isothermal data of experimental nucleation rate as function of supersaturation are compared; the available measurements of critical supersaturation are not included due to their generally lower precision.

The kinetics of homogeneous nucleation of 1-propanol vapor in helium have been already measured by Kacker and Heist[39] (1985) in a static diffusion cloud chamber, in argon by Strey *et al.*[40] (1986), and by Hrubý *et al.*[41] in a two-piston expansion chamber; 1-propanol in nitrogen by Graßmann and Peters[15] (2002) in a piston-expansion tube; and water-1-propanol binary mixture in argon by Viisanen[42] (1991) in a two-piston expansion chamber.

Experimental data from this study are compared to experimental data of others only at temperature ranges that overlap. It is hard to compare experimental data presented in Fig. 7, because the isotherm 290 K (this work) is the subject of comparison to isotherms 294 K [Strey *et al.*[40] (1986)] and 298 K [Kacker and Heist[39] (1985)]; the isotherm 270 K (this work) is subject of comparison to 275 K [Strey *et al.*[40] (1986)], 276 K (Kacker and Heist[39] (1985)], and to best fits

TABLE III. S_{nucl} is supersaturation at T_{nucl}, T_{nucl} is nucleating temperature, p_{tot} is total pressure, and n^* is number of molecules in critical cluster. The standard deviation (SD) is the statistical error obtained from isothermal plots. Δn^* is the difference between the critical cluster sizes from the nucleation theorem Eq. (1) and the Kelvin equation (2).

S_{nucl}	T_{nucl}	p_{tot} (kPa)	n^*	SD	n^* (K)	Δn^*
2.71	290	180	67	0.2	109.6	−42.6
2.73	290	120	84	0.2	107.2	−23.2
2.56	290	50	61.2	0.2	131.4	−70.2
2.99	280	120	69.3	0.1	100.4	−31.1
2.93	280	50	66.1	0.1	105.8	−39.7
3.22	270	25	52.8	0.1	99.2	−46.4
3.65	260	20	59	0.2	88.4	−29.4

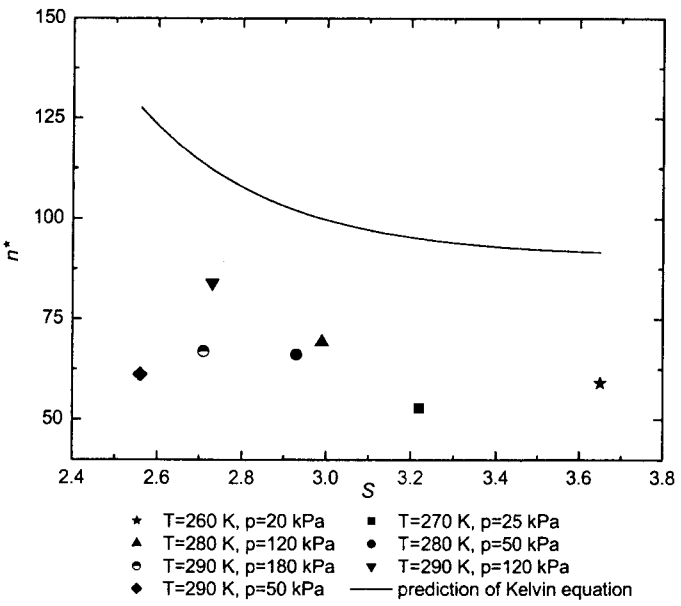

FIG. 5. Molecular content of the critical cluster n^* of 1-propanol as a function of supersaturation S taken from the middle of each isothermal measurement. The symbols represent experimental values; the solid line is prediction of the Kelvin equation.

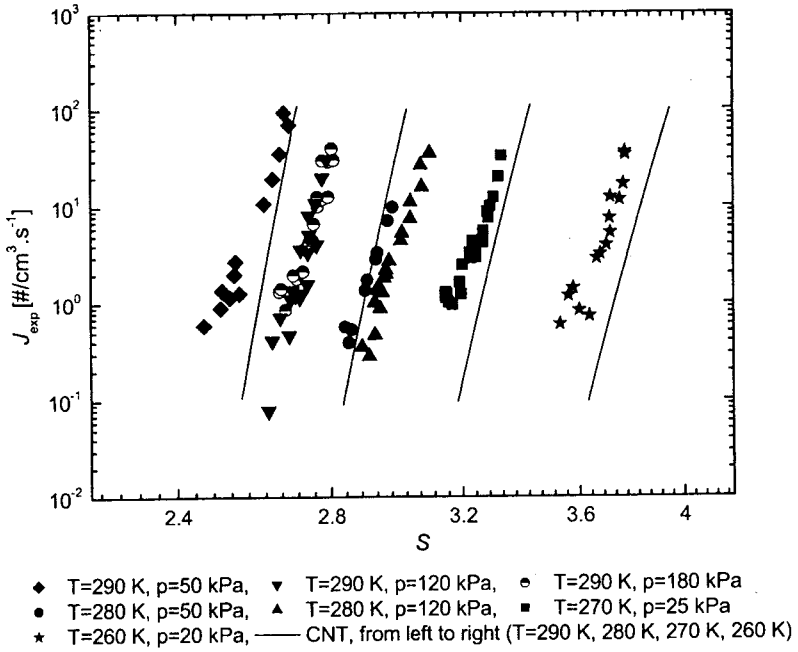

FIG. 6. The experimental nucleation rates of 1-propanol (symbols) and values predicted by CNT (lines) as a function of supersaturation.

to isotherm 272.5 K [Graßmann and Peters[15] (2002)]; and the isotherm 260 K (this work) is subject of comparison to best fits to isotherms 262.6 and 260.9 K [Graßmann and Peters[15] (2002)]. Only isotherm 260 K of Viisanen[42] (1991) and Hrubý *et al.*[41] is directly comparable to this work. In order to compare the experimental data from all available techniques in a consistent manner, the so-called Hale plot was used [Hale[43] (1986), Hale[44] (1992), Hale[45] (2005), and Gharibeh *et al.*[46] (2005)]. Hale suggested a scaled model with the following nucleation rate expression:

$$J_{\text{scaled}} = J_{0c} \exp\left(\frac{16\pi}{3}\Omega^3\left[\frac{T_c}{T} - 1\right]^3 \frac{1}{(\ln S)^2}\right), \tag{3}$$

where J_{0c} is the inverse thermal wavelength cubed per second, evaluated at critical point, and was set to $J_{0c} = 10^{26}$ cm^{-3} s^{-1}.

The Hale plot produces two parameters $C_0[(T_c/T) - 1]^3/(\ln S)^2$ and Ω. The first parameter simultaneously accounts for the temperature and supersaturation dependence in

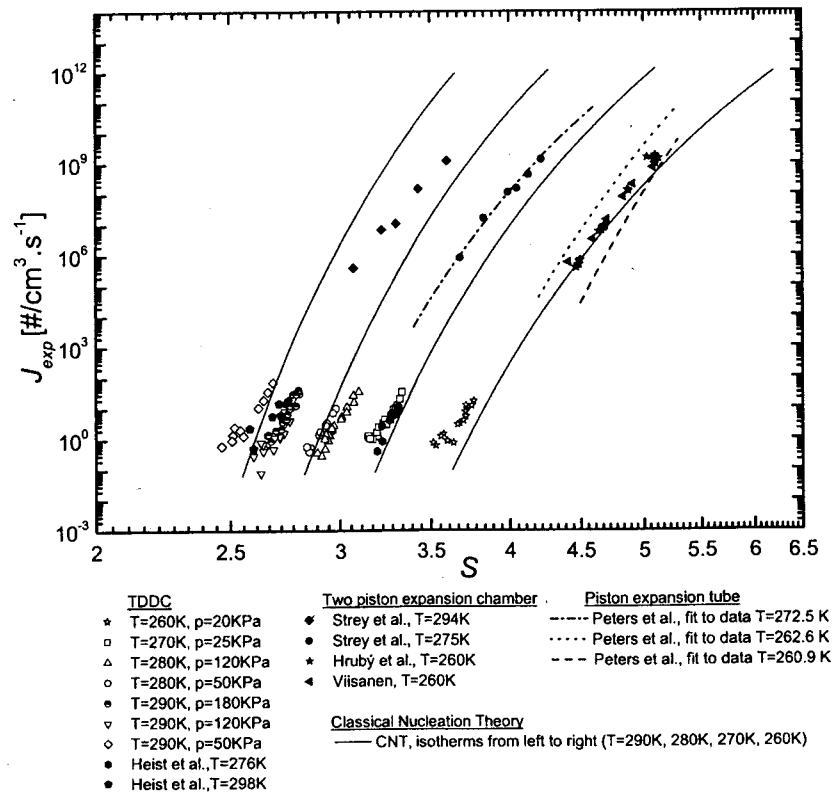

FIG. 7. A comparison of homogeneous nucleation rates J_{exp} of 1-propanol as a function of supersaturation S measured with various devices. All the open symbols are the experimental data from this study; solid symbols, dashed, dotted, and dash-dotted lines are data of others.

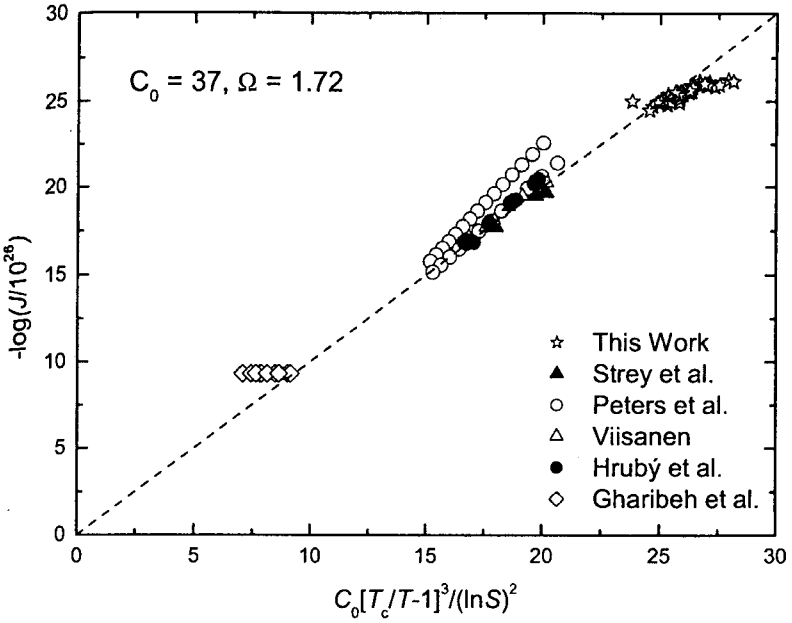

FIG. 8. A comparison of scaled nucleation rates of 1-propanol as a function of scaled supersaturation in a "Hale plot." Only data obeying condition $T/T_c < 0.5$ are presented, i.e., isotherms lower than 270 K.

the exponent of the nucleation rate expression. The Ω is the excess surface entropy per molecule (divided by k) and is estimated from experimental values of the surface tension. The effective value of Ω can be derived from C_0 by

$$\Omega = \left(\frac{3C_0}{16\pi} \ln 10 \right)^{1/3}. \quad (4)$$

This method offers a way to check the experimental data for consistency and also provides basis to compare experimental nucleation rates of any magnitude measured at arbitrary temperature and supersaturation.

The Hale plot given in Fig. 8 uses the same data sets as above but only isotherms obeying Hale's condition $T/T_c < 0.5$ are plotted; plus the data set of Gharibeh *et al.*[46] (2005) from supersonic nozzle measurements at much lower temperatures (T_{nucl}=207–239 K) is included to increase the range of the plot. The compared rates scale well over a wide range of temperature and supersaturation and experimental data from this work seem to be consistent with data of others. The resulting value for parameter C_0 is 37 and the effective value of Ω is 1.72. The experimental value of Ω is ~20% higher than the value derived from fit to the physical property data where Ω_{fit}=1.43.

Pressure effect

Since the influence of the total pressure on experimental nucleation rate was observed repeatedly through recent years and the two-dimensional model is not able to clear up the shift in results carried out at different pressure levels, a separate series of experiments was made to better understand this issue.

It was the aim of these experiments to measure the dependence of nucleation rate on the total pressure only. The experiments were carried out at the isotherm 290 K which offered the widest range of total pressures. One experiment (i.e., one steady state) was performed at a selected pressure. In the next experiment the total pressure was changed. Then the temperatures of plates were readjusted in such a way that after recalculating the profiles (using 1D model of transport processes), the supersaturation corresponding to the vertical position of isotherm 290 K remained approximately the same as in the first experiment. In this way the whole available range of total pressures was mapped. Many experiments were done for this purpose and only those experiments satisfying the condition of nearly constant supersaturation were chosen, Fig. 9. The three ranges of supersaturation (2.75±0.02, 2.78±0.02, and 2.77±0.02) correspond to three different data sets in three time periods. In addition, the first two measurements were done before cleaning and reassembling the chamber and the third measurement was done afterwards to check the reproducibility of the experiments. It should be remembered that the change of 0.02 in supersaturation is a bit less than 1% and that a 3% change in supersaturation usually means the change of one order in magnitude considering nucleation rate at constant temperature.

The experimental nucleation rates as a function of total pressure in the TDCC can be seen in Fig. 10; the data of three data sets are summarized in Tables IV–VI. The decrease of nucleation rate is most pronounced at low total pressures; at higher ones the dependence flattens.

Error analysis to pressure effect

As the decrease of total pressure in the chamber leads to an increase of vapor flux and hence to changes in the thickness of the liquid films on the plates, we attempted to estimate the uncertainty that can be caused by the incorrect determination of the liquid film thickness from the digital images. The determination of the liquid film thickness is an inherent part of the method and needed for the determination of boundary conditions on the surfaces of the liquid films.

We have calculated how large the uncertainty in the determination of the liquid film thickness would have to be to force the highest point of the first data set (solid circles) in Fig. 10, 29 drops cm^{-3} s^{-1} and 44 kPa, to fall on the same line with the experimental points obtained at pressures around the atmospheric pressure. The calculated point is em-

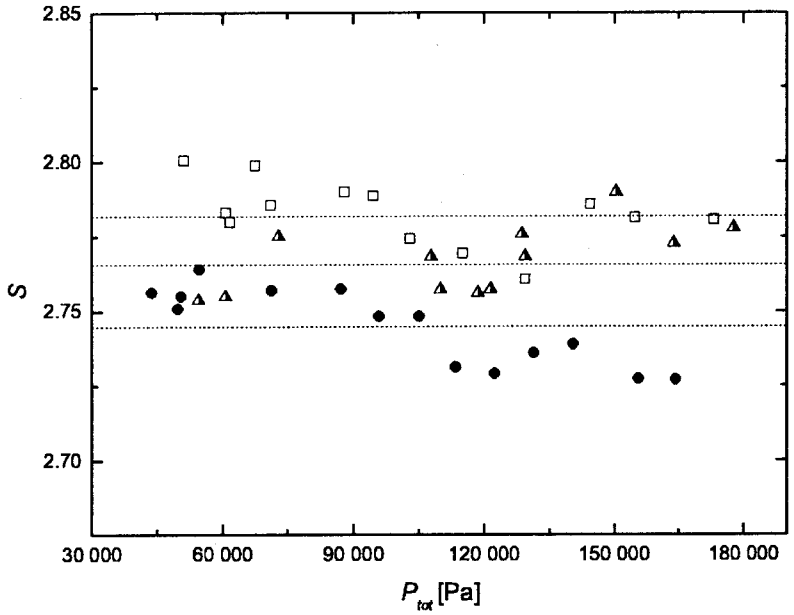

FIG. 9. The supersaturation S as a function of total pressure p_{tot} in the TDCC. Supersaturation corresponds to the position of the isotherm 290 K at which the nucleation rate was determined. The solid circles and the open squares are from first and second data sets (before chamber cleaning and reassembling) and the half-right filled triangles are from third data set (after chamber cleaning and reassembling). The experimental conditions are given in Tables IV–VI.

bedded in Fig. 10 as a solid star and the result of calculation is that the determination of liquid film thickness should fail by about 24 pixels, which corresponds to the error in film thickness of about 1 mm. Such a large uncertainty is highly unlikely, considering that regular experiments were carried out usually with liquid film thickness substantially less than 1 mm. Consequently, results of this detailed experiment further strengthen the hypothesis that the observed pressure effect is real and not an experimental artifact of the method.

CONCLUSIONS

Homogeneous nucleation kinetics in supersaturated vapors of 1-propanol was studied in this paper with helium as a carrier gas. A standard method of a static diffusion chamber was used and the nucleation rate was determined by digital photography with subsequent image analysis. This method makes it possible to determine the nucleation rate independent of any nucleation theory. The dependence of nucleation rate on supersaturation was determined at four isotherms: 290, 280, 270, and 260 K. The 290 K isotherm was studied at three levels of total pressure 50, 120, and 180 kPa and the isotherm 280 K at pressures 50 and 120 kPa. Our results confirmed the results from previous studies in static diffusion chambers, i.e., that the observed nucleation rate increases with a decrease of total pressure. The observed increase was larger in the case of the isotherm 290 K compared to the 280 K isotherm.

In this paper an attempt was made to explain the observed pressure effect by implementing a recently developed two-dimensional model of coupled mass, heat, and momentum transport inside the chamber. The idea behind was pretty simple: If the assumptions on which the frequently used one-dimensional model is based were not fulfilled, i.e., if the heated chamber wall influences the transport processes significantly reaching even into the central part of the chamber, then the vertical profiles of temperature and supersaturation predicted by the 1D model are incorrect. If this were the case, the measured local nucleation rates were related to gen-

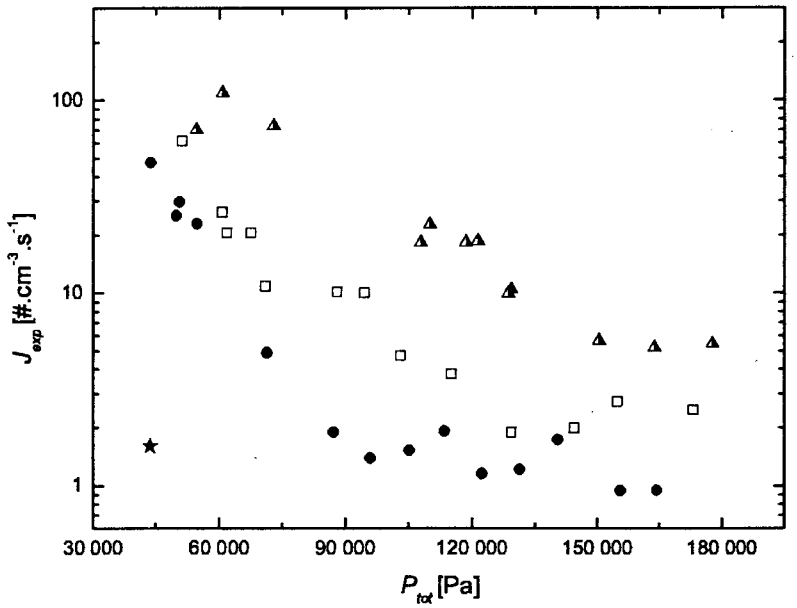

FIG. 10. The experimental nucleation rates J_{exp} of three data sets measured in three different time periods as a function of total pressure p_{tot} in the TDCC (points correspond to the points in Fig. 9). The solid circles, the open squares, and the half-right filled triangles represent the experimental values. The star denotes the uncertainty that would have to be implemented to the determination of liquid film thickness to force the highest point of the first data set (solid circles), 29 drops cm^{-3} s^{-1} and 44 kPa, to fall on the same line with the experimental points obtained at pressures above atmospheric. The experimental conditions are given in Tables IV–VI.

TABLE IV. A detailed study of the pressure effect; experimental data of the first data set. T_b is temperature of bottom plate, T_t is temperature of top plate, T_{nucl} is nucleation temperature, p_{tot} is total pressure, S_{nucl} is supersaturation at T_{nucl}, and J_{exp} is experimental nucleation rate.

T_b (K)	T_t (K)	T_{nucl} (K)	p_{tot} (kPa)	S_{nucl}	J_{exp} (cm^{-3} s^{-1})
321.25	277.18	290	50.478	2.76	9.57*E*0
321.70	276.87	290	71.251	2.76	3.25*E*0
321.79	276.47	290	87.059	2.76	1.84*E*0
321.92	276.47	290	95.786	2.75	1.44*E*0
322.04	276.37	290	105.057	2.75	1.62*E*0
322.03	276.37	290	113.466	2.73	1.12*E*0
322.11	276.30	290	122.284	2.73	1.14*E*0
322.20	276.16	290	131.33	2.74	1.22*E*0
322.31	276.10	290	140.39	2.74	1.73*E*0
322.34	276.04	290	155.454	2.73	9.45*E*−1
322.36	275.96	290	164.27	2.73	9.49*E*−1
320.67	276.28	290	54.535	2.76	1.06*E*1
320.18	276.06	290	49.729	2.75	1.09*E*1
320.76	276.89	290	43.691	2.76	2.91*E*1

erally incorrect values of temperature and supersaturation. And more than that, as the total pressure is one of the key parameters influencing the behavior of the chamber, processing of measured data by the 2D model may led to the explanation of the observed pressure effect.

So, the 2D model was applied, and its results were compared to the results of the 1D model. It could be shown that the heated chamber wall influences even the central part of the chamber. However, this influence (in our range of experiments) was not strong, e.g., at the isotherm 290 K and pressure 50 kPa the use of the 2D model lead to the shift of the isotherm to higher supersaturations by about 0.04 in the supersaturation scale. At the same time, the same isotherm at 20 kPa shifted to the same direction by about 0.01. As a result, the isotherms came a bit closer to each other, but the shift was much smaller than needed in order to explain the pressure effect. This means that the application of the 2D model did not explain the observed pressure effect.

BLE V. A detailed study of the pressure effect; experimental data of the nd dataset. T_b is temperature of bottom plate, T_t is temperature of top te. T_{nucl} is nucleation temperature, p_{tot} is total pressure, S_{nucl} is supersatuon at T_{nucl}, and J_{exp} is experimental nucleation rate.

K)	T_t (K)	T_{nucl} (K)	p_{tot} (kPa)	S_{nucl}	J_{exp} (cm^{-3} s^{-1})
0.67	276.28	290	54.535	2.76	1.06*E*1
0.74	275.91	290	60.578	2.78	2.64*E*1
0.01	275.79	290	67.413	2.80	2.07*E*1
0.27	276.70	290	51.126	2.80	3.31*E*1
0.82	277.11	290	61.671	2.78	2.06*E*1
0.11	277.03	290	70.941	2.79	1.02*E*1
0.45	276.81	290	87.881	2.79	1.01*E*1
0.41	276.61	290	94.385	2.79	1.01*E*1
0.47	276.61	290	102.94	2.77	4.73*E*0
0.65	276.58	290	115.048	2.77	3.78*E*0
0.76	276.52	290	129.312	2.76	1.89*E*0
0.04	276.31	290	144.369	2.79	1.99*E*0
0.09	276.26	290	154.666	2.78	2.73*E*0
0.19	276.14	290	173.082	2.78	2.47*E*0

TABLE VI. A detailed study of the pressure effect; experimental data of the third dataset. T_b is temperature of bottom plate, T_t is temperature of to plate, T_{nucl} is nucleation temperature, p_{tot} is total pressure, S_{nucl} is supersaturation at T_{nucl}, and J_{exp} is experimental nucleation rate.

T_b (K)	T_t (K)	T_{nucl} (K)	p_{tot} (kPa)	S_{nucl}	J_{exp} (cm^{-3} s^{-1})
323.23	277.37	290	110.045	2.76	2.27*E*1
323.29	277.27	290	118.507	2.76	1.84*E*1
322.42	278.21	290	54.474	2.75	7.04*E*1
322.89	277.84	290	72.918	2.77	7.37*E*1
322.44	278.01	290	60.679	2.75	1.09*E*2
323.59	277.65	290	107.901	2.77	1.83*E*1
323.67	277.56	290	121.382	2.76	1.86*E*1
323.81	277.48	290	129.356	2.76	1.04*E*1
323.85	277.43	290	128.627	2.78	9.95*E*0
324.25	277.34	290	150.416	2.79	5.66*E*0
324.19	277.27	290	163.83	2.77	5.22*E*0
324.34	277.20	290	177.677	2.78	5.42*E*0

Another set of experiments was performed with the aim to determine the net influence of total pressure on the nucleation rate. In order to do that, the temperatures of the plates were changed in each subsequent experiment so that the resulting supersaturation corresponding to the height in the chamber where the isotherm 290 K was located was kept constant as well, inside the range of ±0.02. Three sets of data fulfilling this condition were obtained. A result of this exercise is that even in the case when both temperature and supersaturation were kept constant, the nucleation rate was increasing with decreasing total pressure. Moreover, these more detailed experiments showed that the dependence is slightly nonlinear; as total pressure decreases, the pressure effect gets stronger.

The experimental homogeneous nucleation rates of 1-propanol were also compared to theoretical predictions of classical nucleation theory (Becker-Döring-Zeldovich) and with measurements of other investigators. The classical nucleation theory underestimates experimental data of the lower temperature isotherms and overestimates the experimental data of the higher temperature isotherms. The slopes of isotherms are also slightly different.

The predicted values of critical cluster size highly overestimate the values obtained from the slopes of the nucleation rate isotherms. Also the differences among the same isotherms but carried out at different pressure levels can be clearly seen. The highest difference is at isotherm 290 K carried out at 50 kPa; it is about 70 molecules less than that predicted by the Kelvin equation.

The experimental data of this work and data of others compared in "Hale plot" scale well over a wide range of temperature and supersaturation. Based on this comparison, the experimental data from this work seem to be consistent both internally and also with data of others.

ACKNOWLEDGMENT

Support of this work by the Grant Agency of the Academy of Sciences of the Czech Republic (Grant No. IAA2076203) is gratefully acknowledged.

[1] J. Franck and H. G. Hertz, Z. Phys. **143**, 559 (1956).
[2] J. L. Katz, C.-H. Hung, and M. Krasnopoler, *Proceedings of the 12th ICNAA, Vienna 22–27 August 1988* (Springer-Verlag, Berlin, 1988), p. 356.
[3] V. Ždímal, J. Smolík, and H. Uchtmann, J. Aerosol Sci. **26**, 625 (1995).
[4] V. N. Chukanov and B. A. Korobitsyn, Dokl. Akad. Nauk SSSR **307**, 153 (1989).
[5] R. H. Heist, M. Janjua, and J. Ahmed, J. Phys. Chem. **98**, 4443 (1994).
[6] R. H. Heist, M. Janjua, and J. Ahmed, J. Phys. Chem. **99**, 375 (1995).
[7] Y. Viisanen and R. Strey, J. Chem. Phys. **101**, 7835 (1994).
[8] Y. Viisanen, R. Strey, and H. Reiss, J. Chem. Phys. **99**, 4680 (1993).
[9] P. van Remoortere, C. Heath, P. E. Wagner, and R. Strey, in *Proceedings of the 14th International Conference on Nucleation and Atmospheric Aerosols, Helsinki, 26–30 August 1996*, edited by M. Kulmala and P. E. Wagner (Pergamon, Oxford, 1996), p. 256.
[10] M. P. Anisimov, K. M. Anisimov, I. V. Gribanov, R. Y. Zamarayev, N. N. Nalimova, and Y. I. Povolyaev, Colloid J. **56**, 407 (1994).
[11] A.-P. Hyvärinen, D. Brus, H. Lihavainen, V. Ždímal, and H. Uchtmann, Book of Abstracts, European Aerosol Conference 2005, Gent, Belgium, 28 August–2 September 2005, edited by W. Maenhaut, pp. 583.
[12] C. C. M. Luijten, K. J. Bosschaart, and M. E. H. van Dongen, J. Chem. Phys. **106**, 8116 (1997).
[13] C. C. M. Luijten, P. Peeters, and M. E. H. van Dongen, J. Chem. Phys. **111**, 8524 (1999).
[14] C. C. M. Luijten and M. E. H. van Dongen, J. Chem. Phys. **111**, 8535 (1999).
[15] A. Graßmann and F. Peters, J. Chem. Phys. **116**, 7617 (2002).
[16] I. J. Ford, J. Aerosol Sci. **23**, 447 (1992).
[17] D. W. Oxtoby and A. Laaksonen, J. Chem. Phys. **102**, 6846 (1995).
[18] D. Kashchiev, J. Chem. Phys. **104**, 8671 (1996).
[19] V. M. Novikov, O. V. Vasil'ev, and H. Reiss, Phys. Rev. E **55**, 5743 (1997).
[20] A. L. Itkin, Chem. Phys. **238**, 273 (1998).
[21] V. V. Levdanski, J. Smolík, V. Ždímal, and P. Moravec, Int. J. Heat Mass Transfer **45**, 3831 (2002).
[22] V. Ždímal, Ph.D. thesis, Institute of Chemical Technology, Prague, 1998.
[23] J. A. Fisk and J. L. Katz, J. Chem. Phys. **104**, 8649 (1996).
[24] A. Bertelsmann and R. H. Heist, J. Chem. Phys. **106**, 610 (1997).
[25] F. T. Ferguson and J. A. Nuth, J. Chem. Phys. **111**, 8013 (1999).
[26] F. T. Ferguson, R. H. Heist, and J. A. Nuth, J. Chem. Phys. **115**, 10829 (2001).
[27] F. Stratmann, V. Ždímal, M. Wilck, and J. Smolík, J. Aerosol Sci. **30**, 75 (1999).
[28] F. Stratmann, M. Wilck, V. Ždímal, and J. Smolík, J. Phys. Chem. B **105**, 11641 (2001).
[29] V. Ždímal and J. Smolík, Atmos. Res. **46**, 391 (1998).
[30] D. Brus, A.-P. Hyvärinen, V. Ždímal, and H. Lihavainen, J. Chem. Phys. **122**, 214506 (2005).
[31] J. L. Katz and B. J. Ostermier, J. Chem. Phys. **47**, 478 (1967).
[32] J. Smolík and V. Ždímal, Aerosol Sci. Technol. **20**, 127 (1994).
[33] J. Katz, J. Chem. Phys. **52**, 4733 (1970).
[34] A. Bertelsmann and R. H. Heist, J. Chem. Phys. **106**, 610 (1997).
[35] A. Bertelsmann and R. H. Heist, J. Chem. Phys. **106**, 624 (1997).
[36] D. Kashchiev, J. Chem. Phys. **76**, 5098 (1982).
[37] M. P. Anisimov and A. G. Cherevko, Izv. Akad. Nauk. SSR, Ser. Khi. **2**, 15 (1983).
[38] R. Becker and W. Döring, Ann. Phys. (Leipzig) **24**, 719 (1935).
[39] A. Kacker and R. H. Heist, J. Chem. Phys. **82**, 2734 (1985).
[40] R. Strey, P. E. Wagner, and T. Schmeling, J. Phys. Chem. **84**, 2325 (1986).
[41] J. Hrubý, P. E. Wagner, and R. Strey (unpublished).
[42] Y. Viisanen, Ph.D. thesis, University of Helsinki, 1991; Commentationes Physico-Mathematicae et Chemico-Medicae **133**, 37 (1991).
[43] B. N. Hale, Phys. Rev. A **33**, 4156 (1986).
[44] B. N. Hale, Metall. Trans. A **23A**, 1863 (1992).
[45] B. N. Hale, J. Chem. Phys. **122**, 204509 (2005).
[46] M. Gharibeh, K. Yoojeong, U. Dieregweiler, B. E. Wyslouzil, D. Ghosh, and R. Strey, J. Chem. Phys. **122**, 1 (2005).
[47] B. E. Poling, J. M. Prausnitz, and J. P. O'Connell, *The Properties of Gases and Liquids*, 5th ed. (McGraw-Hill, Singapore, 2000).
[48] R. C. Reid, J. M. Prausnitz, and B. E. Poling, *The Properties of Gases and Liquids*, 4th ed. (McGraw-Hill, New York, 1987).
[49] C. L. Yaws, Chem. Eng. (Rugby, U.K.) **22**, 153 (1976).
[50] R. Strey and T. Schmeling, Ber. Bunsenges. Phys. Chem. **87**, 324 (1983).
[51] T. Schmeling and R. Strey, Ber. Bunsenges. Phys. Chem. **87**, 871 (1983).
[52] C. H. Hung, M. J. Krasnopoler, and J. L. Katz, J. Chem. Phys. **90**, 1856 (1989).
[53] J. Vašáková and J. Smolík, Rep. Ser. Aerosol Sci. **25**, 1 (1994).